Rev. Roum. Sci. Techn.– Électrotechn. et Énerg.
Vol. 63, *1*, pp. 52–57, Bucarest, 2018

Dedicated to the memory of Academician Andrei Țugulea

A NEW HYBRID ALGORITHM FOR PHOTOVOLTAIC MAXIMUM POWER POINT TRACKING UNDER PARTIAL SHADING CONDITIONS

AMMAR AL-GIZI[1, 2], AURELIAN CRACIUNESCU[1], MUSTAFA ABBAS FADEL[2], MOHAMED LOUZAZNI[3]

Key words: Photovoltaic (PV), Maximum power point tracking (MPPT), Partial shading conditions.

In this paper, a new hybrid algorithm for photovoltaic (PV) maximum power point tracking (MPPT) under partial shading conditions is proposed. This algorithm is a mix between conventional perturb and observe (P&O) and fuzzy logic control (FLC) PV MPPT algorithms. The main idea of the proposed algorithm is starting MPPT with P&O and switching to FLC algorithm when the transient operating point is close to the global maximum power point (MPP). According to simulation results, in comparison with individual P&O and FLC MPPT algorithms, by using the proposed MPPT algorithm, more energy can be harvested.

1. INTRODUCTION

For partially shaded photovoltaic (PV) systems of more than two series-connected PV cells, the short-circuit current of the shaded cell is less than that of the unshaded cell owing to partial shading caused by passing clouds, tree leaves, dust, or bird dropping, etc. However, the voltage of the shaded cell is overloaded and subjected to the current of all remaining cells, resulting in probable damage to the overall PV module due to a hot spot formation and an increasing in thermal power loss. The overload voltage and hot spot phenomenon can be significantly prevented by parallel-connecting bypass diode across each cell or group of series-connected cells. Moreover, the bypass diode permits the current of the remaining cells to flow through the shaded cell. For reducing the cost, the bypass diode is connected across a group of serially-connected cells instead of a single cell. However, in this case, the group sensitivity to the partial shading will be increased when any cell in the group is locally shaded [1, pp. 127–166].

In contrast, multiple power peaks on the power-voltage (*P–V*) characteristic of the PV system is resulted due to the presence of the bypass diode and shading conditions of individual cells or modules [2].

In the literature, under uniform solar irradiation condition across all solar cells of the PV module, a unique MPP can be detected by a conventional perturb and observe (P&O) and incremental conductance (InC) maximum power point tracking (MPPT) algorithms [3–7].

Both P&O and InC algorithms may have difficulty finding the optimum when used in large arrays where multiple local maxima occur. Recently, new categories which are based on artificial intelligence methods have become popular and are receiving more attention among researchers [8]. These methods consist of several branches such as artificial neural networks (ANNs), fuzzy logic (FL) and the interfacing artificial neural networks with fuzzy logic (ANFIS) [9, 10]. A comparison of different global MPP techniques based on meta-heuristic algorithms for PV system subjected to partial shading conditions has been presented in [11, 12]. Also, several soft computing algorithms which identify the global MPP of the PV system under partial shading conditions, are proposed in [13–15].

In this paper, a model of a PV string consisting of two identical series-connected PV modules is considered. Moreover, the effect of partial shading conditions on the current-voltage (*I–V*) and power-voltage (*P–V*) characteristics of the PV string is studied. Subsequently, the partial shading effect on the available output power which can be extracted from the PV string have been studied. In the subsequent section, a new hybrid MPPT algorithm is proposed and simulated using the Matlab software. Finally, the performances of the proposed hybrid MPPT algorithm are compared with the performances of a fuzzy logic control (FLC) and classical P&O MPPT algorithms in respect of transient and steady state tracking responses.

2. PV SYSTEM UNDER PARTIAL SHADING CONDITIONS

In Fig. 1, a PV string of two series-connected PV modules, unequally illuminated is shown. Each module is protected by a bypass diode. In our system, a stand-alone PV system as in [16] is considered. The PV string instead of a single PV module is used. In the simulation, the PV string consists of two BP SX150S PV modules.

The electrical characteristics of the utilized PV module at standard test condition (STC) are depicted in Table 1 [16].

One of the PV modules is fully illuminated by solar irradiation level of 1 000 W/m^2 (unshaded) and another PV module is illuminated by different solar irradiation levels: 700 W/m^2, 500 W/m^2, and 300 W/m^2; that is equivalent to partial shading conditions of 30 %, 50 %, and 70%, respectively.

Table 1

Electrical characteristics of BP SX150S PV module at STC

Parameter	Value
Maximum power (P_{max})	150 W
Voltage at P_{max} (V_{mpp})	34.5 V
Current at P_{max} (I_{mpp})	4.35 A
Short-circuit current ($I_{sc} = I_{ph}$)	4.75 A
Open-circuit voltage (V_{oc})	43.5 V
Temperature coefficient of I_{sc}	(0.065 ± 0.015) %/ ^{O}C
Temperature coefficient of V_{oc}	-(160 ± 20) mV/ ^{O}C

The partial shading conditions can be expressed as:

[1] 'Politehnica' University of Bucharest, Electrical Engineering Faculty, Romania, E-mail: ammar.ghalib@yahoo.com
[2] Al-Mustansiriyah University, Faculty of Engineering, Baghdad, Iraq
[3] Mathematics, Information and Applications Team, National School of Applied Sciences, Abdelmalek Essaadi University, Tanger, Morocco

$$Shading\ Condition = \frac{1000 - irradiation}{1000} \times 100\ \% . \qquad (1)$$

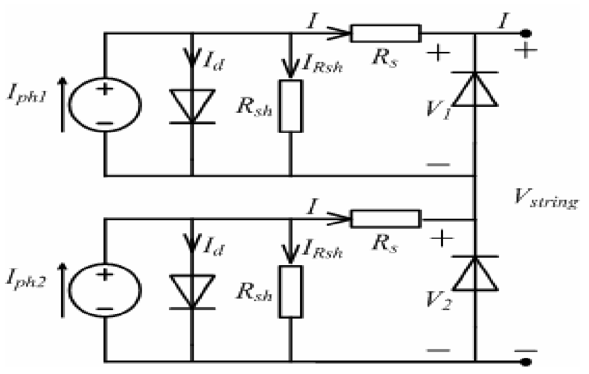

(a)

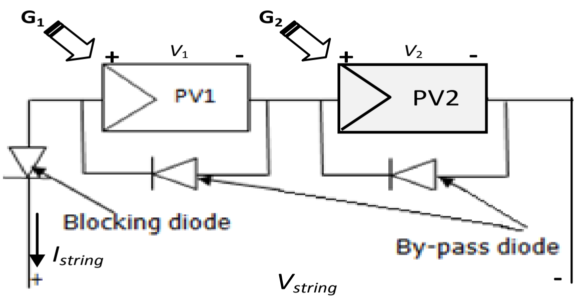

(b)

Fig. 1 – PV string of two identical PV modules connected in series: a) circuit diagram; b) block diagram.

The current and voltage of the PV string under partial shading conditions can be calculated by the following equations [17]:

$$I = \begin{cases} I_{ph1} - I_o\left(\exp\left(\dfrac{q(V_1 + IR_s)}{N_s n KT}\right) - 1\right) - \left(\dfrac{V_1 + IR_s}{R_{sh}}\right) & I \geq I_{ph2} \\ I_{ph2} - I_o\left(\exp\left(\dfrac{q(V_2 + IR_s)}{N_s n KT}\right) - 1\right) - \left(\dfrac{V_2 + IR_s}{R_{sh}}\right) & I < I_{ph2} \end{cases} \qquad (2)$$

$$V = \begin{cases} V_1 & I \geq I_{ph2} \\ V_1 + V_2 & I < I_{ph2} \end{cases} . \qquad (3)$$

I_{ph1} and I_{ph2} are the photocurrent or short-circuit current of the two modules, illuminated by irradiation G_1 and G_2, respectively. R_s and R_{sh} are the series and shunt resistances of a single solar cell. I_o is the diode's reverse saturation current, q is the electron charge (1.602×10^{-19} C), K is the Boltzmann's constant (1.381×10^{-23} J/K), n is the diode ideality factor, N_s is the number of serially-connected solar cells inside each PV module, and T is the junction temperature of the PV cell. V_1 and V_2 are the voltages of the unshaded and shaded PV modules, respectively. I and V are the current and voltage of the utilized PV string, respectively [17].

Since I_{ph1} is greater than I_{ph2}, at short-circuit condition of the PV string, the current of the unshaded module will bypass the shaded module through the conductive bypass diode2, hence the PV string current and voltage are I_{ph1} and V_1, according to (2). By the time, when the current of the unshaded module becomes less than I_{ph2} due to the increase in the load voltage, the current of the shaded module will bypass the unshaded module through the conductive bypass diode1, according to (2).

The dependency of the reverse saturation current (I_o) on the cell temperature (T) can be illustrated as:

$$I_o = I_{or} \times \left(\frac{T}{T_r}\right)^3 \times \exp\left(\frac{q\,E_g}{n\,K}\left(\frac{1}{T_r} - \frac{1}{T}\right)\right). \qquad (4)$$

E_g is the band gap energy of the semiconductor used in the cell. I_{or} and T_r are the reverse saturation current and cell temperature at STC, respectively. Whereas, the short-circuit current of the i_{th} module (I_{phi}) based on the solar irradiation (G_i) and cell temperature (T_i), can be expressed by:

$$I_{phi} = \frac{G_i}{Gr}\left(I_{scr} + \alpha(T_i - T_r)\right). \qquad (5)$$

I_{scr} and G_r are the short-circuit current and solar irradiation at STC, respectively. α is the coefficient of short circuit current temperature.

Subsequently, the *I-V* and *P-V* characteristics of the PV string under different shading conditions and constant cell temperature of 25 °C, are shown in Fig. 2. It can be seen from Fig. 2, the presence of local and global maximum power points (MPPs) rather than a unique MPP due to a non-uniform irradiation levels across the two modules in the PV string and the presence of bypass diodes connected across each module.

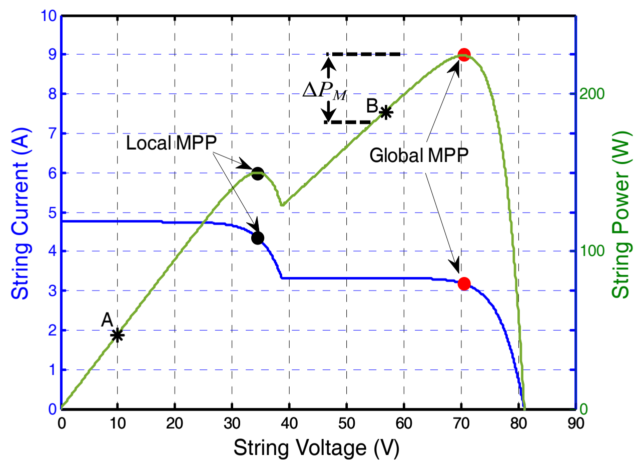

(a)

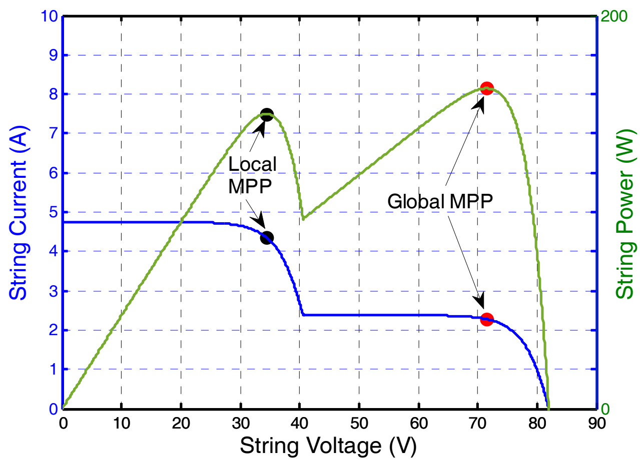

(b)

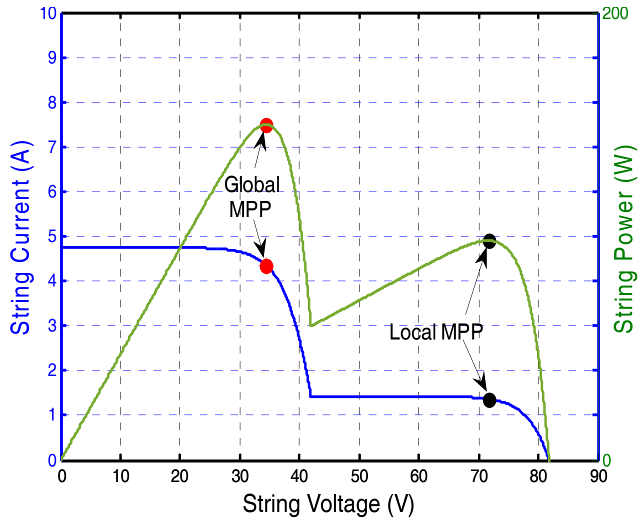

(c)

Fig. 2 – *I-V* and *P-V* characteristics of a partially shaded PV string at a cell temperature of 25 °C; a) one of PV modules is shaded by 30%; b) one of PV modules is shaded by 50%; c) one of PV modules is shaded by 70%.

Furthermore, Fig. 3 reveals the partial shading effect on the PV string output power on the local and global MPPs. The power difference between these MPPs is decreased by increasing the shading condition until the value of 54% and significantly increased by increasing the shading condition again, as shown in Fig. 3.

Table 2 summaries this effect.

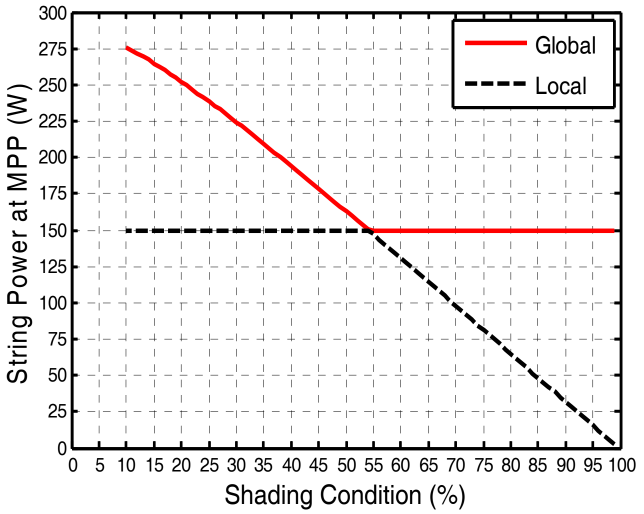

Fig. 3 – PV string power at MPPs under different shading conditions.

Table 2

Effect of partial shading conditions on the PV string power

Shading condition	*Local MPP power* [W]	*Global MPP power* [W]	*String power difference* [W]
30 %	149.98	224.32	74.34
50 %	149.98	163	13.02
70 %	98.02	149.98	51.96

Subsequently, an efficient MPPT algorithm is necessary to track the global MPP and to avoid the trapping in the local MPP.

3. PROPOSED HYBRID MPPT ALGORITHM

The PV system which uses the proposed hybrid MPPT algorithm is shown in Fig. 4.

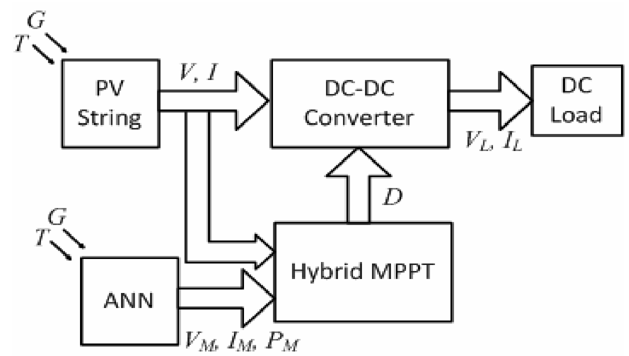

Fig. 4 – PV system with the proposed MPPT algorithm.

The proposed hybrid MPPT algorithm is a combination of two algorithms: P&O and FLC. When the operating point is located far away from the global MPP (point A in Fig. 2a), a large constant perturbation step (ΔD) is used to close the desired MPP with a minimum rising time during the transient tracking region. However, a variable ΔD is decided by using FLC MPPT algorithm when the operating point closes the global MPP (point B in Fig. 2a). In the meantime, the power difference between the global MPP and the operating point (ΔP) is less than an allowable power difference (ΔP_M). The value of ΔD is continuously decreased based on the FLC rule-base (RB) during this stage until reaching a minimum value at the global MPP. Although the tracking speed is decreased, a minimum oscillation is satisfied at the steady state region. The allowable power difference is selected in such a way to improve the transient and steady state tracking performances. The flow chart of the proposed hybrid MPPT algorithm is depicted in Fig. 5.

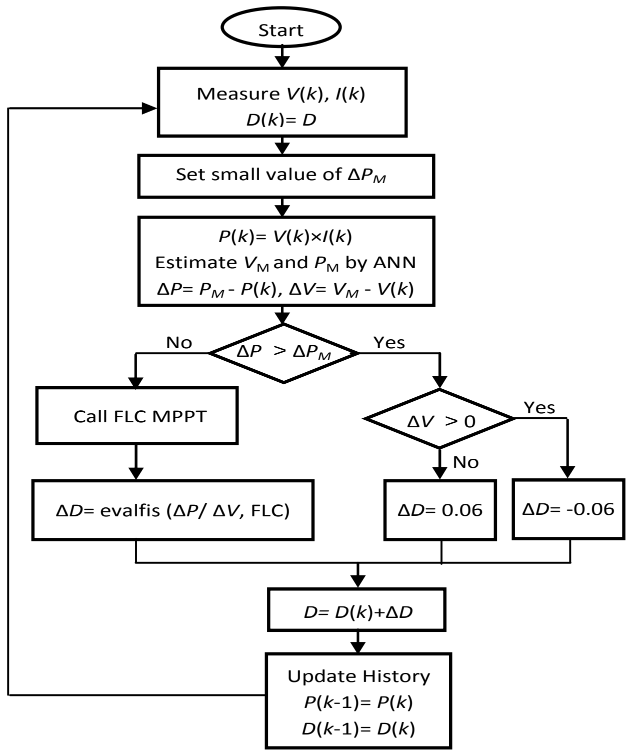

Fig. 5 – Flow chart of the proposed hybrid MPPT method.

The following subsections explain the FLC MPPT algorithm and ANN which is used to predict the values of voltage (V_M), current (I_M), and a corresponding power (P_M) at the global MPP.

3.1. ARTIFICIAL NEURAL NETWORK (ANN) TRAINING

To predict the global MPP of the PV string under different partial shading conditions, a three-layers ANN developed in [18] have been used.

The Matlab instructions, used for training the ANN, are listed below:

$$P = [G; T];$$

$$V_{\text{ref}} = [V_M];$$

```
net= newff ([0 1;15 35], [20 1],{'tansig' 'purelin'},'trainlm');
net.trainParam.epochs= 500;
net.trainParam.goal= 0.00025;
net= train (net,P,Vref);
```

"newff" instruction is used to define the layers number, a number of neurons in the hidden layer, and the activation function.

Moreover, the differentiable performance function (mean squared error – MSE) is used to measure the performance of the ANN training process. The training performance is illustrated in Fig. 6.

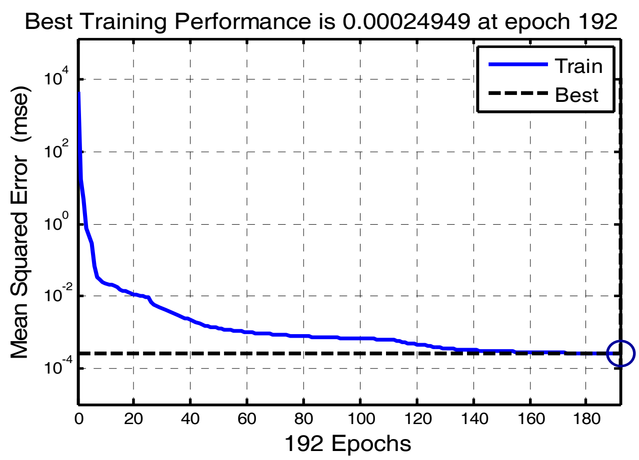

Fig. 6 – The training performance of ANN.

3.2. FUZZY LOGIC CONTROL (FLC)

The FLC is used to produce a variable suitable ΔD during the tracking process. In this paper, the FLC has one input and one output. The FLC input at sampling k can be written as:

$$\frac{\Delta P}{\Delta V}(k) = \frac{P_M(K) - P(K)}{V_M(K) - V(K)}. \tag{6}$$

$V(k)$ and $P(k)$ are the instantaneous PV string's voltage and power, respectively, whereas, $V_M(k)$ and $P_M(k)$ are the predicted PV string's voltage and power at the global MPP. The change in a duty ratio $\Delta D(k)$ represents the FLC output at sampling k.

The main processes of FLC are fuzzification, inference engine, and defuzzification [3]. In the fuzzification, the asymmetrical FLC of five triangular membership functions (MFs) for both input and output variables are used. The FLC input and output MFs are shown in Fig. 7. The asymmetrical FLC is adopted due to its advantage over the symmetrical FLC type [19]. The fuzzy subsets MFs are labeled by the linguistic terms; negative big (NB), negative small (NS), zero (Z), positive small (PS), and positive big (PB).

Since each one of the input and output of the FLC contains five MFs, the IF-THEN fuzzy rule-base table can be composed by using five fuzzy rules in the inference engine process. The rule-base table of asymmetrical FLC is shown in Table 3.

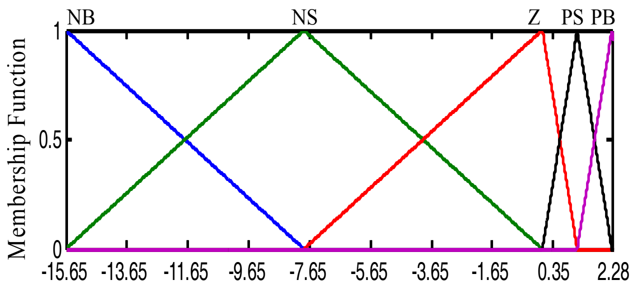

(a)

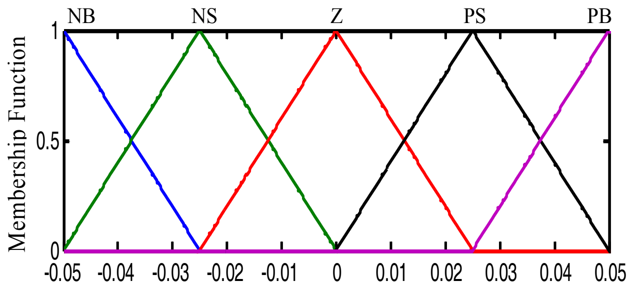

(b)

Fig. 7 – MFs of asymmetrical FLC; a) Input $\Delta P/\Delta V$; b) Output ΔD.

Table 3

Rule-base table of asymmetrical fuzzy logic controller

$\Delta P / \Delta V$	NB	NS	Z	PS	PB
ΔD	PB	PS	Z	NS	NB

The final process of the FLC is the defuzzification. This process is used to extract a real value of the output ΔD from its fuzzy value using a well-known center of gravity (COG) method which is based on the union of all rules' outputs as [3, 16, 19]:

$$\Delta D = \frac{\sum_{i=1}^{n} \Delta D_i \times \mu(\Delta D_i)}{\sum_{i=1}^{n} \mu(\Delta D_i)}. \tag{7}$$

ΔD is the real value of the change in duty ratio. Hence, the final real value of D(k) for the dc-dc converter which produced by the FLC MPPT can be expressed by:

$$D(K) = D(K-1) + \Delta D(K). \tag{8}$$

4. SIMULATION RESULTS AND DISCUSSION

The performances of the proposed hybrid PV MPPT algorithm are evaluated and compared with the FLC and conventional P&O MPPT algorithms under constant cell temperature of 25 °C and unequal irradiation levels of

1 000 W/m^2 and 500 W/m^2 across the two modules of the PV string, knowing that the classical P&O algorithm presented in [5–7, 16] is used. These performance results are compared in terms of; recognizing the global MPP, rising time to reach the global MPP, average extractable power (P_{av}) at the steady state, and the amount of available harvested energy (energy yield) from the PV system during 10 s of the simulation time.

The traces of PV string operating point on the *P-V* curves based on the P&O, FLC, and hybrid MPPT algorithms are illustrated in Fig. 8. The operating point is started on the left side of the *P–V* curves, assuming an initial *D* of 0.95. However, Figs. 9 and 10 depict the power and energy which can be extracted from the PV string, respectively.

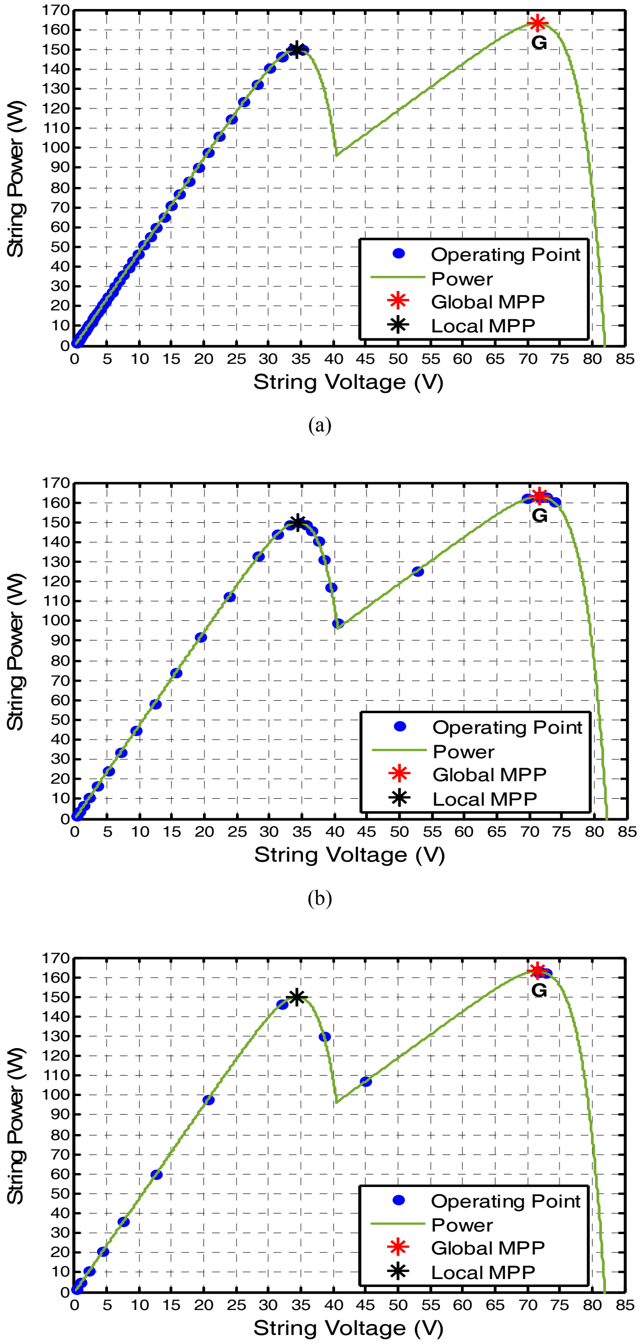

(c)

Fig. 8 – *P-V* characteristics of PV string and traces of operating point under 50 % of shading conditions, using; a) P&O MPPT algorithm; b) FLC MPPT algorithm; c) hybrid MPPT algorithm.

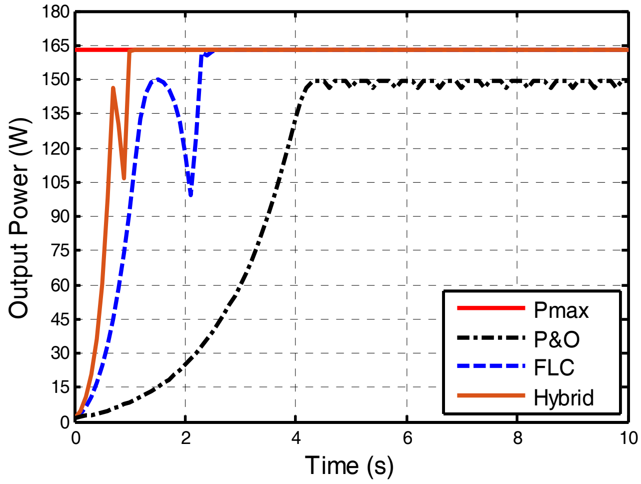

Fig. 9 – *P-V* string output power using MPPT algorithms under 50 % of shading condition.

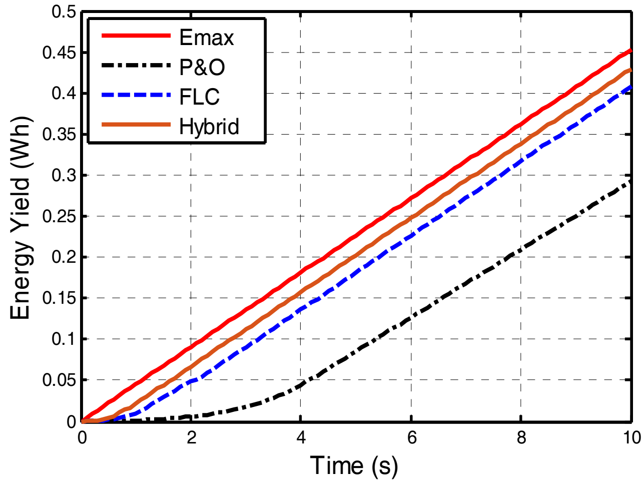

Fig. 10 – *P-V* string energy yield using MPPT algorithms under 50 % of shading conditions.

It is clear from Fig. 8a, the operating point based on P&O MPPT algorithm is trapped in the local MPP. Meanwhile, a fluctuating power around this point with an average value of 148.9 W is extracted, due to the constant perturbation duty ratio (ΔD) of 0.01, as shown in Fig. 9. However, the FLC and hybrid MPPT algorithms can successfully reach the global MPP, extracting an average power of 159.9 W and 162.9 W, as shown in Figs. 8 and 9, respectively. Moreover, the tracking response based on the hybrid MPPT algorithm is faster than the FLC MPPT algorithm with rising time of 1 s and 2.3 s, respectively, as shown in Fig. 9.

The amelioration of the proposed hybrid MPPT algorithm is distinct due to the usage of variable perturbation step ΔD during the tracking algorithm. A large constant value of ΔD is used in the beginning stage of the tracking process when the operating point is located away from the global MPP, like a P&O algorithm. The main idea of the proposed hybrid PV MPPT algorithm is to switch from P&O to FLC algorithm when the operating point reaches the allowable region, close the global MPP, meanwhile, the proposed algorithm decreases ΔD until reaching the global MPP with less oscillation, as shown in Figs. 8 and 9. Knowing that the global MPPT of 163 W is predicted based on the ANN.

Subsequently, the proposed hybrid MPPT algorithm can harvest the most energy from the PV system during 10 s, as shown in Fig. 10. The energy yield based on P&O, FLC and hybrid MPPT algorithms are 0.29 Wh, 0.41 Wh, and 0.43 Wh, respectively. Knowing that, the ideal energy yield from the PV string during 10 s is 0.453 Wh.

Table 4 summarizes the comparison results based on the three utilized MPPT algorithms.

Table 4

Comparative results of MPPT methods under 50 % of shading conditions

Parameter	*P&O*	*FLC*	*Hybrid*
Average steady-state power, P_{av}[1] [W]	148.9 (Local)	159.9 (Global)	162.9 (Global)
Rising time, t_r [s]	-	2.3	1
Energy yield[2] [Wh]	0.29	0.41	0.43

[1] Ideal PV string power at global MPP is 163 W.
[2] Ideal energy yield during 10 s is 0.453 Wh.

5. CONCLUSIONS

Under partial shading conditions, a multiple MPPs appeared as a result of unequally irradiation across the PV modules and due to the existence of bypass diodes across each PV module. Consequently, the necessity for an efficient tracking algorithm is increased.

From the simulation results, the conventional P&O MPPT algorithm trapped in the local MPP, as shown in Fig. 8a. However, FLC and the proposed hybrid MPPT algorithms can successfully detect the global MPP, as shown in Fig. 8b and Fig. 8c, respectively.

The proposed hybrid algorithm can quickly reach the global MPP with less oscillation, as shown in Fig. 9, thereby extracting more average power than the FLC PV MPPT algorithm, 162.9 W instead of 159.9 W, respectively, as depicted in Table 4. According to the improvements in terms of transient and steady state tracking responses, the proposed hybrid MPP algorithm can harvest more solar energy from the PV system than the other MPPT algorithms, as shown in Fig. 10, where, the energy yield using the proposed hybrid, FLC, and P&O MPPT algorithms are 0.43 Wh, 0.41 Wh, and 0.29 Wh, respectively, as illustrated in Table 4.

ACKNOWLEDGMENTS

The first author thanks the Iraqi government represented by the Ministry of higher education and scientific research, Al-Mustansiriya University, Baghdad, Iraq for their financial support.

Received on November 7, 2017

REFERENCES

1. H. Häberlin, *Photovoltaics system design and practice*, John Wiley & Sons, 2012, pp. 127–166.
2. C.S. Chin, P.,Neelakantan, S.S. Yang, B.L. Chua, K. Tze Kin Teo, *Effect of Partially Shaded Conditions on Photovoltaic Array's Maximum Power Point Tracking*, International Journal of Simulation-Systems, Science & Technology, **12**, *3* (2011).
3. A. Attou, A., A. Massoum, M. Chadli, *Comparison study of two tracking methods for photovoltaic systems*, Rev. Roum. Sci. Techn.– Électrotechn. et Énerg, **60**, *2*, pp. 205–214 (2015).
4. P.S. Sikder, P. Nital, *Incremental conductance based maximum power point tracking controller using different buck-boost converter for solar photovoltaic system*, Rev. Roum. Sci. Techn.–Électrotechn. et Énerg, **62**, *3*, pp. 269–275 (2017).
5. A.G. Al-Gizi, S.J. Al-Chlaihawi, *Study of FLC based MPPT in comparison with P&O and InC for PV systems*, International Symposium on Fundamentals of Electrical Engineering (ISFEE), pp. 1–6 (2016).
6. A.G. Al-Gizi, *Comparative study of MPPT algorithms under variable resistive load*, International Conference on Applied and Theoretical Electricity (ICATE), pp. 1–6 (2016).
7. A. Al-Gizi, S. Al-Chlaihawi, A. Craciunescu, *Efficiency of Photovoltaic Maximum Power Point Tracking Controller Based on a Fuzzy Logic, Advances in Science, Technology and Engineering Systems Journal (ASTES)*, **2**, *3*, pp. 1245–1251 (2017).
8. M. Seyedmahmoudian, B. Horan, T.K. Soon, R. Rahmani, A.M.T. Oo, A. Stojcevski, *State of the art artificial intelligence-based MPPT techniques for mitigating partial shading effects on PV systems – A review*, Renew. Sustain. Energy Rev., **64**, pp. 435–455 (2016).
9. M. Nabipour, M. Razaz, S. G. Seifossadat, S. S. Mortazavi, *A new MPPT scheme based on a novel fuzzy approach*, Renew. Sustain. Energy Rev., **74**, pp. 1147–1169 (2017).
10. F. Belhachat, C. Larbes, *Global maximum power point tracking based on ANFIS approach for PV array configurations under partial shading conditions*, Renew. Sustain. Energy Rev., **77**, pp. 875–889 (2017).
11. S. Titri, C. Larbes, K.Y. Toumi, K. Benatchba, *A new MPPT controller based on the ant colony optimization algorithm for Photovoltaic systems under partial shading conditions*, Appl. Soft Comput., **58**, pp. 465–479 (2017).
12. H. Rezk, A. Fathy, A.Y. Abdelaziz, *A comparison of different global MPPT techniques based on meta-heuristic algorithms for photovoltaic system subjected to partial shading conditions*, Renew. Sustain. Energy Rev., **74**, pp. 377–386 (2017).
13. K. Ishaque, Z. Salam. *A review of maximum power point tracking techniques of PV system for uniform insolation and partial shading condition*. Renewable and Sustainable Energy Reviews, **19**, pp. 475–488 (2013).
14. Z. Salam, J. Ahmed, B.S. Merugu, *The application of soft computing methods for MPPT of PV system: A technological and status review*, Applied Energy, **107**, pp. 135–148 (2013).
15. N. Hashim, Z. Salam, S.M. Ayob, *Maximum power point tracking for stand-alone photovoltaic system using evolutionary programming*, 8th IEEE International Power Engineering and Optimization Conference (PEOCO), pp. 7–12 (2014).
16. A.M. Othman, M.M. El-arini, A. Ghitas, A. Fathy, *Realworld maximum power point tracking simulation of PV system based on fuzzy logic control*, NRIAG Journal of Astronomy and Geophysics, **1**, *2*, pp. 186–194 (2012).
17. M. Seyedmahmoudian, S. Mekhilef, R. Rahmani, R. Yusof, E.T. Renani, *Analytical modeling of partially shaded photovoltaic systems*, Energies, **6**, *1*, pp. 128–144 (2013).
18. A.G. Al-Gizi, A. Craciunescu, S.J. Al-Chlaihawi, *The use of ANN to supervise the PV MPPT based on FLC*, 10th International Symposium on Advanced Topics in Electrical Engineering (ATEE), pp. 703–708 (2017).
19. A. Al-Gizi, S. Al-Chlaihawi, A. Craciunescu, *Comparative study of some FLC-based MPPT methods for photovoltaic systems*, MATTER, International Journal of Science and Technology, **3**, *3*, pp. 36–50 (2017).